



Optimization of a multi-moderator neutron spectrometer for use in epithermal neutron spectrum measurements in BNCT

Zeinab Kazemi¹, Faezeh Rahmani^{1,a} , Nima Ghal-Eh², Sergey V. Bedenko³

¹ Department of Physics, K. N. Toosi University of Technology, P. O. Box 16315-1618, Tehran, Iran

² Department of Physics, School of Science, Ferdowsi University of Mashhad, P. O. Box 91775-1436, Mashhad, Iran

³ National Research Tomsk Polytechnic University, P.O. Box 634050, Tomsk, Russian Federation

Received: 4 February 2025 / Accepted: 30 April 2025

© The Author(s), under exclusive licence to Società Italiana di Fisica and Springer-Verlag GmbH Germany, part of Springer Nature 2025

Abstract In boron neutron capture therapy (BNCT), it is crucial to accurately measure the neutron energy spectra within the therapeutic range. To achieve this, a variety of instrumentations, both real-time and passive, has been utilized for energy spectrum measurement during or prior to the treatment. However, a significant challenge arises from the abundance of epithermal neutrons in the BNCT neutron energy spectrum, coupled with the narrow therapeutic energy interval. To overcome this challenge, dedicated systems need to be designed to ensure precise measurements. This article focuses on a comprehensive study that explores the feasibility of designing and optimizing a cylindrical multi-moderator neutron spectrometer. Ultimately, this study is able to improve the results of previous efforts by 56.6%. The study utilizes a LiI(Eu) thermal neutron detector, which is based on the thermal beam derived from the beam shaping assembly of the Tehran Research Reactor, which serves as the exclusive neutron source for the BNCT in Iran. Also, the AFITBUNKI code is employed for neutron energy spectrum unfolding.

1 Introduction

Boron neutron capture therapy (BNCT) represents a promising approach in treating various cancers, notably brain tumors, through the selective capture of neutrons by boron-10 (^{10}B) compounds [1]. In this therapeutic method, a biologically targeted ^{10}B compound is administered and localized within the tumor site after injection [2]. Subsequently, a beam of epithermal neutrons, tailored to the depth of the tumor, is directed at the affected region [3]. The interaction of ^{10}B with thermal neutrons yields ^7Li and alpha particles. These products, characterized by their limited ranges and large deposition energies at the interaction site, effectively induce the destruction of tumor cells [4].

Epithermal neutrons employed to treat deep-seated tumors, and thermal neutrons for superficial tumors or cancer cells, depending on the tumor depth [5]. The International Atomic Energy Agency (IAEA) has set forth some recommended specifications for the neutron spectrum used in BNCT. These guidelines provide essential criteria or an ideal neutron beam used in BNCT, as outlined in Table 1 [6].

The precise measurement of the therapeutic neutron energy spectrum and the evaluation of gamma-ray contamination within this spectrum are essential prerequisites for successfully implementing BNCT. At present, the TRR stands as the exclusive source providing the therapeutic neutron spectrum adhering to the rigorous standards set forth by the IAEA [7].

Numerous methodologies are available for measuring and characterizing the neutron spectrum for the BNCT. In 2020, Rahmani et al. introduced an initial design for a multi-moderator spectrometer dedicated to neutron measurements in the BNCT [8]. While simulation results employing the Monte Carlo code (MCNP) demonstrated satisfactory outcomes, the need for enhancing the spectrometer precision in the BNCT measurements was apparent [9].

In light of this necessity, this study delves into the measurement of the therapeutic neutron spectrum, employing an unfolding methodology in a well-suited multi-moderator neutron spectrometry framework for BNCT. Furthermore, this work introduces a novel mechanism for potential future research endeavors.

The therapeutic spectrum employed in the BNCT is characterized by a predominance of epithermal neutrons within a narrow energy range from 1 eV to 10 keV. To address this, the researchers have opted to leverage the principles of multi-moderator spectrometers, drawing inspiration from the design of the well-known Bonner Spheres [10].

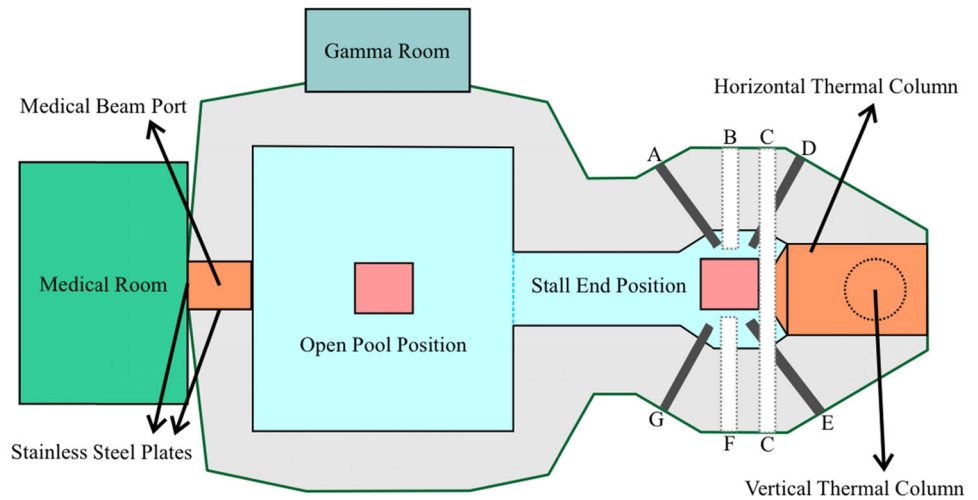
The Bonner spheres method involves using a set of spheres, each composed of distinct neutron-moderating materials, enabling the measurement of a comprehensive energy spectrum ranging from thermal neutrons to several GeV neutrons. Within this detection system, each polyethylene sphere houses a central thermal neutron detector, such as LiI(Eu), BF_3 , or ^3He detector [11].

^a e-mail: FRahmani@kntu.ac.ir (corresponding author)

Table 1 The IAEA recommendation specifications for the neutron spectrum used in BNCT [6]

Neutron beam parameter	Recommended value
Flux of epithermal neutrons ($\text{cm}^{-2} \text{s}^{-1}$)	$> 10^9$
Gamma dose rate to epithermal neutron flux (Gy.cm^2)	$< 2 \times 10^{-16}$
Fast neutron dose rate to epithermal neutron flux (Gy.cm^2)	$< 2 \times 10^{-16}$
Fast neutron group energy	Higher than 10 keV
Epithermal neutron group energy	From 1 eV to 10 keV
Thermal neutron group energy	Less than 1 eV

Fig. 1 The TRR with the beam delivery channel and thermal columns [7]



One notable advantage of the Bonner spheres method, in addition to its favorable response function, is its ability to minimize the influence of gamma rays. This is achieved through the dependency of neutron detection on particle reactions with high Q-values, facilitating the effective discrimination of gamma-rays [12].

2 Materials and methods

The exclusive neutron source employed to date for the experimental studies within this approach is nuclear reactors capable of producing the requisite neutron spectrum.

2.1 TRR

The TRR, a pool-type research reactor operating at 5 MW, employs low-enriched uranium fuel plates. It features seven beam tubes of varying sizes and geometries, alongside a thermal column equipped with removable graphite blocks (Fig. 1).

To facilitate the BNCT, a BSA is normally suggested for the installation at the thermal column of TRR. This BSA comprises moderators, filters, reflectors, and collimators, aiming to optimize neutron flux characteristics for BNCT [13].

At the exit window of the thermal column, a therapeutic neutron beam expected to deliver an estimated epithermal flux of $6.5E8 \text{ n/cm}^2 \cdot \text{s}$, catering to medical applications [14].

For the accurate acquisition and comprehensive understanding of this spectrum, Fig. 2 provides a visual representation of the final treatment spectrum at the TRR reactor's output and its associated spectrum shaper, facilitating subsequent comparisons and validation of unfolded spectra for the future analyses.

The primary objective of this investigation is the precise measurement of the energy spectrum of the TRR employing LiI(Eu)-based detection setup. However, despite satisfactory of previous simulation results using the MCNP Monte Carlo code, there exists a need to enhance the spectrometer accuracy to ensure its suitability for the BNCT measurements.

In this cylindrical detector configuration, multiple high-density polyethylene (HDP) cylindrical layers are incorporated to moderate and attenuate fast and epithermal neutrons, together with a thermal neutron detector at the center of the assembly.

To ensure the effective detection of the neutron energy spectrum, characterized by a dominant flux in the epithermal energy range, a series of well-suited moderator layers are positioned in front of the central detector.

As mentioned, this study introduces the proposed spectrometer structure, as depicted in Fig. 3, to improve the precision of epithermal neutron energy spectrum measurement for the BNCT applications. The designed detector proposed in this study consists

Fig. 2 The neutron energy spectrum obtained from the TRR [8]

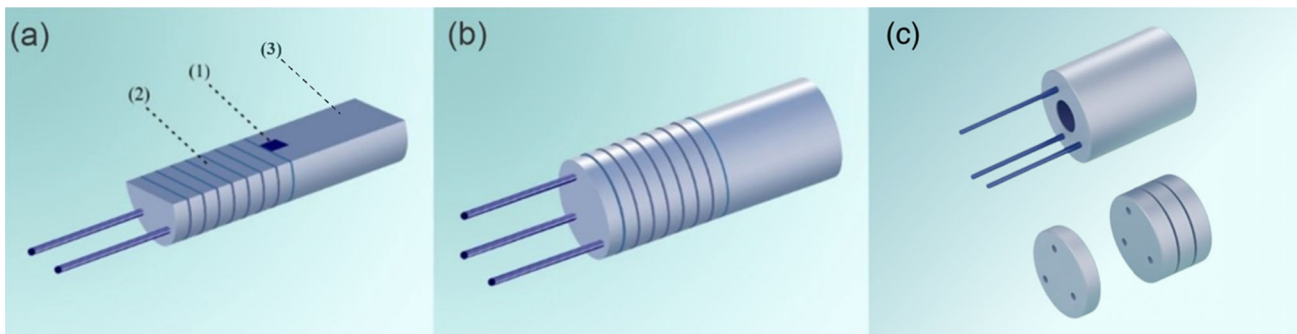
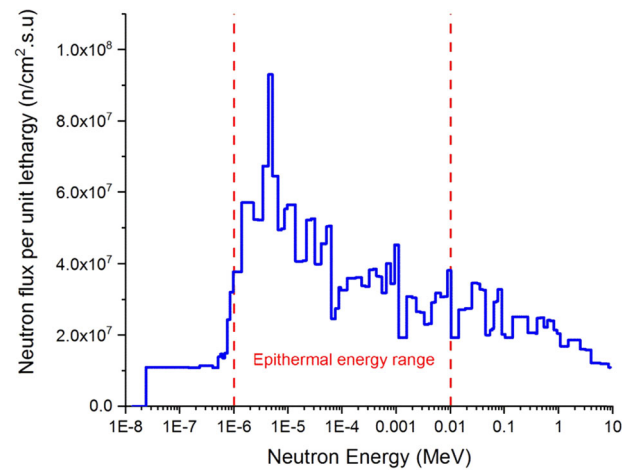


Fig. 3 The schematic view of the proposed design of the spectrometer. **a** A cross-sectional view **b** full view **c** Separate detector components (1) LiI(Eu) detector at the center of the spectrometer, (2) Variable polyethylene moderator layers, (3) Fixed part (The dimensions are not scaled)

of a central LiI(Eu) detector, modeled as a small cylinder with a radius and height of 1 cm which is positioned in the front side of polyethylene moderator with radius and height of 10 cm and 10 cm, respectively, which shown as a fixed part of the designed spectrometer. Also, cylindrical polyethylene moderator layers (20 layers) are positioned in front of it, in which each layer has a thickness of 0.5 cm and a radius of 10 cm. A cross-sectional view of this configuration is shown in Fig. 3.a.

The full view of structure is shown in Fig. 3.b, which comprises a fixed part that holds the central detector in place, while the moderator layers are mounted onto stationary rods, as illustrated in Fig. 3.c. By successively adding moderator layers, a multi-moderator spectrometer with a defined total thickness is formed.

2.2 Preparation of detector response matrix

In this research, the LiI(Eu) crystal as the central detector in the proposed setup was selected due to its high thermal neutron detection efficiency and suitability for compact dimensions [15]. To optimize neutron slowing down, the polyethylene moderator layers are placed close to the detector owing to their inherent simplicity and effectiveness in moderating neutrons.

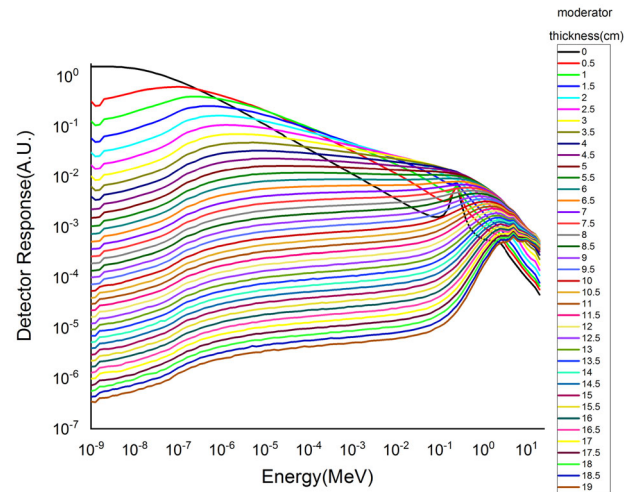
The initial step involves determining the minimum thickness of the LiI(Eu) detector necessary to effectively moderate the highest energy neutrons within the therapeutic spectrum, accomplished through simulation with the Monte Carlo code MCNP [16]. The specific range of this requisite thickness is detailed in Table 2, with the minimum moderator thickness established at 9 cm. Subsequently, the counts recorded by the detector are systematically gathered for diverse neutron energies, encompassing a range of moderator layer thicknesses. These data form the response matrix of this experimental configuration. All data were characterized by uncertainties well below the acceptable value of 10%.

To explain the methods used in this study, we carried out detailed simulations using the Monte Carlo code MCNP. These simulations aimed to understand how the central LiI(Eu) detector would respond to different thicknesses of polyethylene moderator when exposed to a range of neutron energies. This led to the creation of a unique response matrix specifically for this research. Notably, this process involved conducting more than 4000 individual simulation runs. Figure 4 shows the detector's response, visualized as a 39×94 array, characterized by uncertainties well below the acceptable value of 10%. This accurately crafted response matrix is an input data utilized for the unfolding of the neutron spectrum, a vital component of the present study.

Table 2 Recorded neutron flux irradiated to the detector behind polyethylene moderators at different thicknesses

Thickness (cm)	Neutron flux (n/cm ² .s) × 10 ⁻⁷	Thickness (cm)	Neutron flux (n/cm ² .s) × 10 ⁻⁷
6.5	3.89	10	4.73
7	4.17	10.5	4.78
7.5	4.47	11	3.98
8	4.27	11.5	4.14
8.5	4.51	12	4.58
9	5.12	12.5	4.09
9.5	4.09	13	4.18

Fig. 4 Simulated count rates recorded by the detector behind different thicknesses of moderators against various neutron energies



2.3 Spectrum unfolding process

The neutron detector responses to various neutron energies are basically determined by parameters such as thickness, material composition, and density, depending on the chosen spectrum unfolding methodology. Generally, if the detector’s response to each specific energy level is figured out, this information can then be used to understand how it is responded to by a wider range of neutron energies. Conversely, in cases where the detector exhibits sensitivity across a wide energy range, the mathematical operation known as spectrum unfolding can be utilized for neutron spectrum prediction [17, 18].

Each polyethylene layer within the setup, including the bare detector, contributes to a count rate, denoted as C in the following equations. C clearly depends on the neutron energy E, the detector response R, and the neutron flux Φ [19]. The use of a first-kind Fredholm integral equation, as evident in Eq. 1 and Eq. 2, offers a formal representation of this relationship:

$$C = \int_{E_i}^{E_f} R(E)\Phi(E)dE \tag{1}$$

$$C = \sum_{j=1}^n R_{ij}\Phi_j, i = 1, m \tag{2}$$

This can be simplified into a matrix form, as shown in Eq. 3.

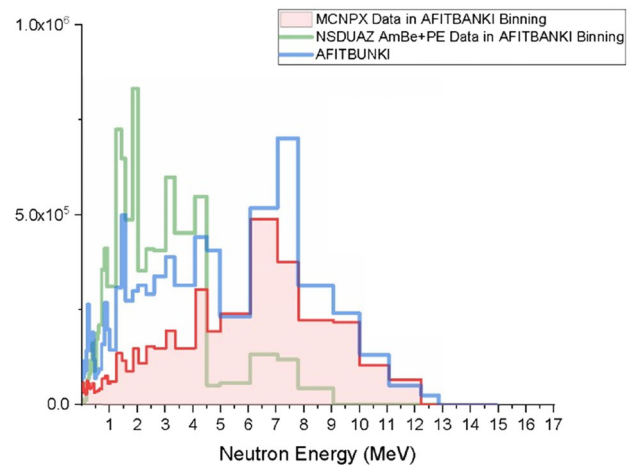
$$M = R\Phi \tag{3}$$

The direct solution of Eq. 1 for $\Phi(E)$ is a challenging task. Consequently, it is a common practice to address this problem by resolving Eq. 3 instead of Eq. 1, where it is accomplished by employing numerical analysis codes. Prominent among these codes are well-established ones such as AFITBUNKI and NSDUAZ, which are widely recognized for their effectiveness in spectrum unfolding.

To ensure the most accurate and reliable results, it becomes imperative to conduct a comparative operational analysis of these two codes. To this end, a concise description of both AFITBUNKI and NSDUAZ is provided, followed by a comprehensive comparison of their results [20, 21].

Fig. 5 Dialog box designed for the unfolding using AFITBUNKI

Fig. 6 The comparison between NSDUAZ, AFITBUNKI, and MCNPX for the unfolding of the ^{241}Am -Be neutron source spectrum. The blue curve represents AFITBUNKI, the green curve represents NSDUAZ, and the red curve represents MCNPX codes, respectively



2.4 AFITBUNKI spectrum unfolding code

The AFITBUNKI spectrum unfolding code is a widely recognized and practical tool, designed for spectrum unfolding and implemented in the FORTRAN programming language. The AFITBUNKI employed here for neutron spectrum unfolding. This code, in an improved version of the original BUNKI code, offers substantial capabilities for spectrum analysis.

The available version of the AFITBUNKI code was developed in FORTRAN 77 and consists of approximately 1500 lines [22]. The original version of the code posed challenges due to its encapsulation of data related to the response functions of Bonner spheres, proposed neutron spectra, flux-to-dose conversion coefficients, and spectrum unfolding algorithm (utilizing the SPUNIT iterative method) all within a single routine. To enhance modifiability and maintain clarity, the code was restructured into a primary routine with 22 subroutines, complemented by a user-friendly interface (as depicted in Fig. 5).

The crucial input parameters for the AFITBUNKI unfolding code encompass the number of spheres and readings per sphere. Moreover, the program offers flexibility by enabling users to incorporate calibration and smoothing coefficients. Users can also specify the number of iterations required to reach an optimal solution. Upon program execution, the resulting neutron energy spectrum is furnished to the user in text file format and as part of the output information.

Following rigorous assessments and comparisons with results obtained from the introduction of two different unfolding codes, the spectrum unfolding was executed for ^{241}Am -Be and ^{252}Cf neutron sources using two separate codes. Subsequently, the application and results of both codes were compared. Ultimately, the AFITBUNKI code was selected for several compelling reasons. Firstly, as illustrated in Fig. 6, it exhibited significantly superior performance in comparative evaluations. Secondly, its open-source nature rendered it amenable to optimization and customization by the research community [23].

Following the selection of the AFITBUNKI code for therapeutic spectrum unfolding, the unfolding process for BNCT was initiated. Initial unfolding results were obtained, but to accommodate the code for therapeutic spectra, an optimization phase was required. During this optimization, each user-determined variable within the program interface underwent refinement.

To ensure a meaningful statistical comparison, the chi-squared test was performed. It is worth noting that the AFITBUNKI code necessitates an initial guess spectrum for the unfolding process. This guess can be a simple unrelated continuous spectrum or, notably, the output therapeutic spectrum from TRR. The latter choice ensures that the final unfolded spectrum closely aligns with the therapeutic spectrum.

Fig. 7 Comparison of the unfolded spectrum using the initial flat spectrum guess

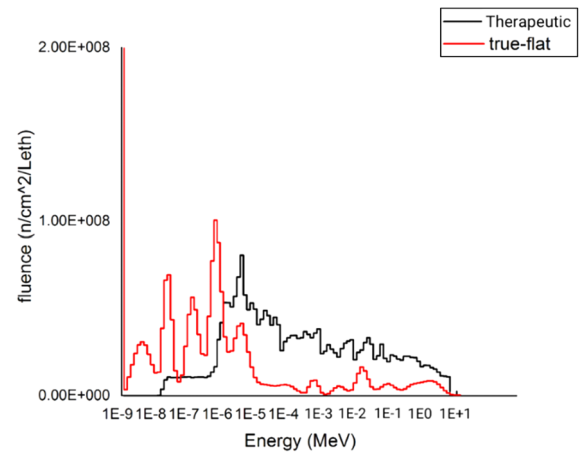
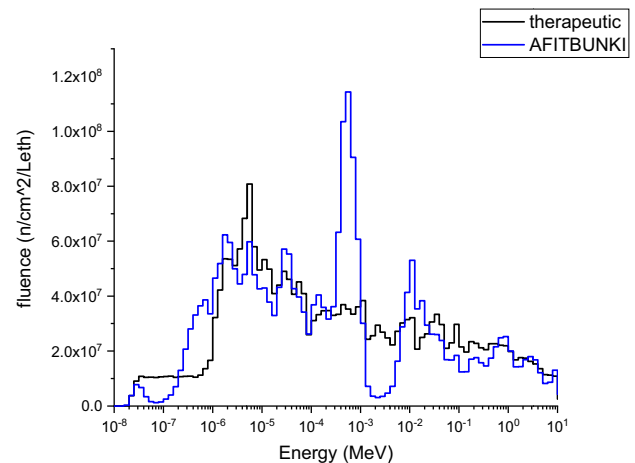


Fig. 8 Comparison of the unfolded spectrum using the therapeutic spectrum as a guess (blue) with the therapeutic spectrum (black)



The influence of the initial estimated spectrum on the unfolding results is clearly demonstrated in the following illustrations. Through systematic adjustment of the variables, as visualized in Fig. 7 to Fig. 10, the unfolding process was carefully conducted, resulting in optimal characteristics.

As it is shown in Fig. 7, the results of AFITBUNKI code when the initial guess is a flat spectrum are compared with the reference therapeutic one.

Subsequently, to promote the simulation results, the TRR therapeutic spectrum was fed into the AFITBUNKI code as an initial guess which showed better agreement (See Fig. 8).

In the next step, the influence of different setting factors given in the dialog box on the unfolding results was investigated. As shown in Fig. 9 the best agreement is seen for the case where the number of iterations before error test and the maximum number of iterations are 1 and 10, respectively.

To check whether the iteration algorithm in the AFITBUNKI code (SPUNIT subroutine) is working properly, the iteration numbers below 10 were examined (See Fig. 10).

Through the careful adjustment of the variables mentioned above, as visualized in Fig. 7 to Fig. 10, the unfolding was performed with optimal precision. Figure 11 provides a vivid depiction of the comparison between the best unfolding results achieved using the AFITBUNKI code and the therapeutic spectrum of TRR.

This study significantly expands on the original work of Rahmani et al., who proposed and optimized the MMNS structure. A crucial part of our work is to compare the spectroscopic results obtained with our approach to those from the previous research. This comparative analysis, illustrated in Fig. 11, confirms the success of the methodology used in the present work.

Fig. 9 Unfolded spectra for various iterations before error tests (left number) and the maximum number of iterations (right number)

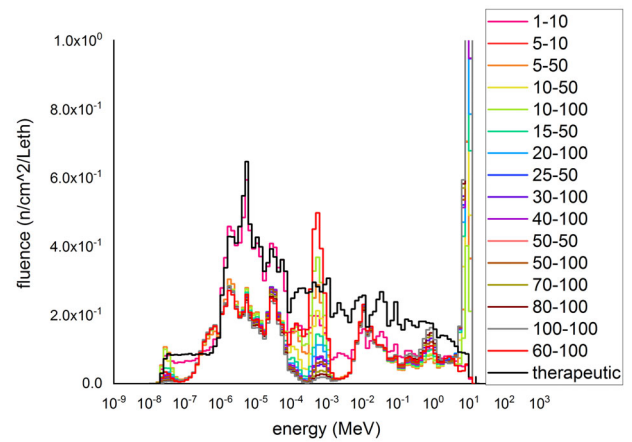


Fig. 10 Unfolded spectra for various iterations before different error tests (left number) and the maximum number of iterations below 10 (right number)

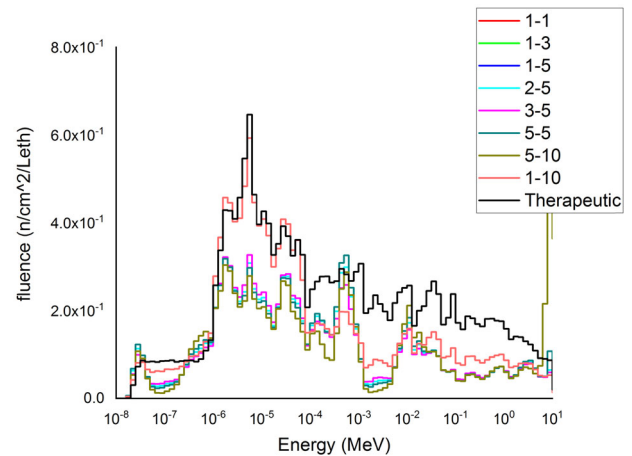
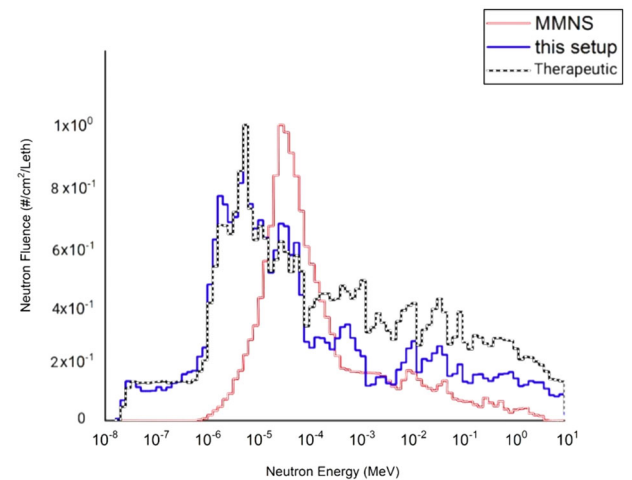


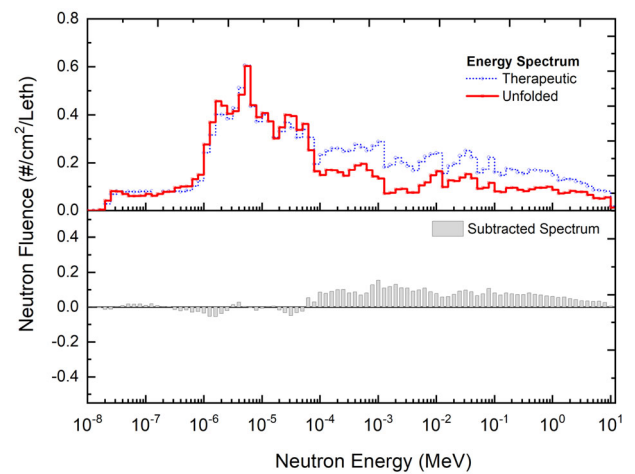
Fig. 11 Comparison between the spectrum obtained from the MMNS (red), the therapeutic spectrum (black), and the spectrum obtained in the present work (blue)



3 Conclusions

The dedicated MMNS methodology proposed in this study was effectively accomplished its primary objective, which was to provide an accurate spectral analysis of the neutron spectrum resulting from the TRR for application in BNCT. Through the optimization of numerous parameters influencing the spectral unfolding process, this methodology has achieved a marked performance improvement compared to its predecessor. The results obtained from this study indicate a 56.6% enhancement over the previous framework, as quantified through the Mean Absolute Percentage Error (MAPE) metric.

Fig. 12 Comparison between the therapeutic spectrum (blue), and the spectrum obtained in the present work (red)



In summary, the neutron spectroscopy methodology presented here proficiently conducts spectral analysis within the therapeutic spectrum range of the TRR, spanning approximately from $10E-8$ to 10 MeV as shown in Fig. 12. These achievements underscore the significance of this research in advancing the capabilities in neutron spectrum analysis for BNCT applications.

Data Availability Statement Data availability based on the request will be provided.

References

- R.F. Barth, J.A. Coderre, M.G.A.H. Vicente, T.E. Blue, Boron neutron capture therapy of cancer: current status and future prospects. *Clin. Cancer Res.* **11**(11), 3987–4002 (2005). <https://doi.org/10.1158/1078-0432.ccr-05-0035>
- A. Wittig et al., Boron analysis and boron imaging in biological materials for boron neutron capture therapy (BNCT). *Crit. Rev. Oncol. Hematol.* **68**(1), 66–90 (2008)
- H.R. Mirzaei et al., Boron neutron capture therapy: moving toward targeted cancer therapy. *J. Cancer Res. Ther.* **12**(2), 520–525 (2016)
- S. González et al., First BNCT treatment of a skin melanoma in Argentina: dosimetric analysis and clinical outcome. *Appl. Radiat. Isot.* **61**(5), 1101–1105 (2004)
- I. Kato et al., Effectiveness of BNCT for recurrent head and neck malignancies. *Appl. Radiat. Isot.* **61**(5), 1069–1073 (2004)
- R. F. During storage, “IAEA TECDOC SERIES”.
- Y. Kasesaz, H. Khalafi, F. Rahmani, Design of an epithermal neutron beam for BNCT in thermal column of Tehran research reactor. *Ann. Nucl. Energy* **68**, 234–238 (2014)
- F. Rahmani, N. Ghal-Eh, H.R. Vega-Carrillo, A multi-moderator neutron spectrometer for use in BNCT studies of the Tehran research reactor. *Appl. Radiat. Isot.* **174**, 109751 (2021)
- D.B. Pelowitz et al., MCNPX 2.7. 0 Extensions, Los Alamos National Laboratory, Los Alamos, NM, LA-UR-11-02295, vol. 4, (2011)
- A. Mitaroff, *Design, calibration and tests of an extended-range Bonner sphere spectrometer* (Tech. U., Atominst, Vienna, 2001)
- D. Thomas, A. Alevra, Bonner sphere spectrometers—a critical review. *Nucl. Instrum. Methods Phys. Res., Sect. A* **476**(1–2), 12–20 (2002)
- C. Birattari, E. Dimovasili, A. Mitaroff, M. Silari, A Bonner Sphere Spectrometer with extended response matrix. *Nucl. Instrum. Methods Phys. Res., Sect. A* **620**(2–3), 260–269 (2010)
- Y. Kasesaz et al., BNCT project at Tehran research reactor: current and prospective plans. *Prog. Nucl. Energy* **91**, 107–115 (2016)
- Y. Kasesaz et al., Design and construction of a thermal neutron beam for BNCT at Tehran research reactor. *Appl. Radiat. Isot.* **94**, 149–151 (2014)
- R. Murray, Use of Li_6I (Eu) as a scintillation detector and spectrometer for fast neutrons. *Nucl. Instrum.* **2**(3), 237–248 (1958)
- L. S. Waters, MCNPX user’s manual, Los Alamos national laboratory, vol. 124, (2002)
- N. Ghal-Eh, M. Kalaei, A. Mohammadi, H. Vega-Carrillo, Replacement of Bonner spheres with polyethylene cylinders for the unfolding of an ^{241}Am -Be neutron energy spectrum. *Appl. Radiat. Isot.* **128**, 292–296 (2017)
- J.M. Gómez-Ros, R. Bedogni, M. Moraleda, A. Romero, A. Delgado, A. Esposito, Design and validation of a single sphere multi-detector neutron spectrometer based on $LiF: Mg, Cu, P$ thermoluminescent dosimeters. *Radiat. Meas.* **45**(10), 1220–1223 (2010)
- V. Mares, H. Schraube, Evaluation of the response matrix of a Bonner sphere spectrometer with LiI detector from thermal energy to 100 MeV. *Nucl. Instrum. Methods Phys. Res., Sect. A* **337**(2–3), 461–473 (1994)
- H. Vega-Carrillo, J. Ortiz-Rodríguez, M. Martínez-Blanco, NSDUAZ unfolding package for neutron spectrometry and dosimetry with Bonner spheres. *Appl. Radiat. Isot.* **71**, 87–91 (2012)
- N. Ghal-Eh, R. Koohi-Fayegh, S. Hamidi, Low-energy neutron flux measurement using a resonance absorption filter surrounding a lithium glass scintillator. *Radiat. Phys. Chem.* **76**(6), 917–920 (2007)
- S.C. Miller, AFITBUNKI: a modified iterative code to unfold neutron spectra from Bonner sphere detector data. in air force INST of tech wright-Pattersonafb oh school of engineering, (1993)
- J. Ortiz R, M. Martinez B, H. Vega C, and E. Gallego, A comparison in the reconstruction of neutron spectrums using classical iterative techniques, (2009)

Springer Nature or its licensor (e.g. a society or other partner) holds exclusive rights to this article under a publishing agreement with the author(s) or other rightsholder(s); author self-archiving of the accepted manuscript version of this article is solely governed by the terms of such publishing agreement and applicable law.